An Advanced STATCOM Model for Optimal Power Flows using Newton's Method

Behzad Kazemtabrizi, *Member, IEEE,* and Enrique Acha, *Senior Member, IEEE*

***Abstract*— This paper presents the OPF formulation of a recent power flow STATCOM model [1]. The new model puts forward an alternative, insightful interpretation of the fundamental frequency operation of the PWM-controlled Voltage Source Converter (VSC), in an optimal fashion. The new model makes provisions for the explicit representation of the converter's internal ohmic and switching losses which in the context of an OPF formulation, yields an optimum operating point at which these power losses are at a minimum. The STATCOM model possesses unparalleled control capabilities in the operational parameters of both the AC and DC sides of the converter. Such control modeling flexibility is at its best when expressed in the context of an OPF solution using Newton's method. The STATCOM equations are incorporated into the OPF formulation using Lagrangian functions in quite a natural manner for efficient optimal solutions using a single frame-of-reference. The inequality constraint set of variables is handled equally well using the multipliers method. The prowess of the new model is demonstrated using two sample systems.**

***Index Terms*-- FACTS, STATCOM, Voltage Source Converter, Optimal Power Flows, Newton's method**

I. INTRODUCTION

LIKE the Static VAR Compensator (SVC), the primary function of the STATCOM is to provide flexible reactive power support at key points of the transmission system but at a faster speed of response and with an enhanced performance [2]. The STATCOM may take the form of one of the many possible converter topologies available today, made up of fully controllable power electronic valves and driven by PWM (or equivalent) control [3]. The most popular switched-mode converter topologies fulfilling the requirements of providing fast voltage support are the two-level and the three-level PWM-driven VSCs, together with the newer Modular Multilevel Converter (MMC) VSCs. They are normally connected to a point of the power grid using a step-up transformer with tap-changing facilities [4]-[7]. The fundamental frequency operational behavior of the VSC, as seen from its AC side, resembles that of a controllable voltage source. Such a characteristic has been exploited to good effect in power system studies to represent the STATCOM as a controllable voltage source behind coupling impedance [8]-[9]. This is not dissimilar to the way in which synchronous condensers are represented in power flow studies. Such a simple concept represents well the fact that at the fundamental frequency, the STATCOM converter's output voltage may be adjusted against the AC system's voltage in the converter to achieve very tight control targets, a capability afforded by the switched-mode converter technology [1]-[9]. Nevertheless, for all its attractiveness this concept fails to explain the operation of the STATCOM from its DC side. Some of the most obvious shortcomings of the STATCOM model based on the equivalent voltage source concept are: (i) there is no easy way to ascertain whether or not the converter's operation is within the linear region of operation [10]; (ii) switching losses tend to be neglected; (iii) the internal ohmic losses of the converter along with the effects of the converter's magnetics are normally lumped together with those of the interfacing transformer which, more often than not, is a tap changer. This has provided the motivation to develop a more realistic STATCOM model for fundamental frequency operation [1]; one which overcomes the limitations of the equivalent voltage source representation and is suitable for assessing the impact of both conventional multi-level and modular multi-level converters (MMC) [11]-[12], on large power networks and in an optimal manner.

This paper may be considered a companion paper of [1] where the conventional power flow solution of the STATCOM model has been put forward. In the OPF problem – which is the subject matter of this paper - a chosen system objective function (or a group of functions) is solved towards its optimum operating point subject to system's realistic operating boundaries.

In the OPF formulation presented in this paper, the system objective function is chosen to be the cost of generators' active power dispatch [13]. It should be noted that the set of results obtained from an OPF solution may not necessarily agree with those obtained from a conventional power flow solution even when applied to the same system. In an OPF solution, the solution space is shaped by the action of different controllers in the system that set the boundaries on control state variables and functions (i.e. nodal active and reactive power flows) [2]. Adhering to the necessary optimality criteria will eventually result in convergence towards a different operating point (optimum) than the one obtained by the conventional power flow calculation. The OPF formulation requires creating a Lagrangian function with appropriate penalty functions to keep the system operating conditions within their acceptable boundaries whilst adhering to the necessary optimality criteria. The reason is that the key part of

B. Kazemtabrizi is with the School of Engineering and Computing Sciences in Durham University. (email: behzad.kazemtabrizi@durham.ac.uk)

E. Acha is with the Department of Electrical Engineering of the Tampere University of Technology (TUT), Finland. (email: enrique.acha@tut.fi)

the optimality criteria found in OPF formulations is not incorporated in the conventional power flow formulation. For instance, and as exemplified by the OPF simulations presented in this paper, the converter's internal switching losses are reduced when compared to those obtained with a conventional STATCOM power flow algorithm.

Optimal solutions of the new STATCOM model yield considerable reductions in power system losses and in the converter's internal power losses, when compared to the solutions furnished by the STATCOM model solved using conventional power flows [1]. Furthermore, optimal solutions with the new STATCOM model will also yield improved solutions compared to the optimal solutions provided by the voltage source representation of the STATCOM, and with less computational complexity.

II. STATCOM NEW MODEL

The equivalent electric circuit for the STATCOM model is shown in Fig.1.

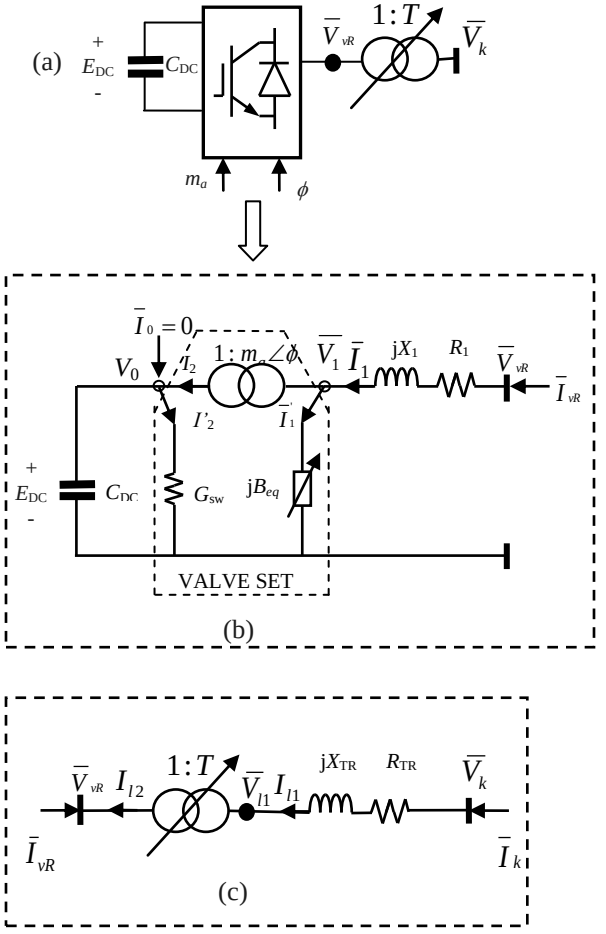

Fig. 1: (a) STATCOM schematic representation; (b) voltage source converter equivalent circuit; (c) on-load tap-changing transformer equivalent circuit

The STATCOM consists of two main components – a voltage source converter (VSC) and a tap-changing coupling transformer (LTC), as illustrated in Fig. 1(a). The VSC is modeled as an ideal complex tap-changing transformer, shown in Fig. 1(b). The reason for using a complex tap changer to model the VSC operation stems from the following fundamental relationship applicable to the PWM controlled operation of the VSC:

$$\bar{V}_1 = m_a^{'} e^{j\varphi} E_{DC} \tag{1}$$

where tap magnitude $m_a^{'}$ of the ideal complex tap-changing transformer corresponds to the amplitude modulation coefficient of an actual two-level, three-phase VSC, defined as $m_a^{'} = (\sqrt{3}/2)m_a$, in which the PWM-controlled VSC operates in the linear range with $0<m_a<1$ [5]. The phase angle ϕ is the phase angle of the complex voltage $\bar{V}_1$ relative to the system phase reference.

It should be noted that such aggregated relationships are also applicable to represent the fundamental frequency operation of three-level, three-phase VSCs driven by PWM control since in this application the interest is in the relationship between E_{DC} and $\bar{V}_1$ through m_a and ϕ. This would be regardless of the number of switches and converter levels.

On the other hand, Modular Multilevel Converters (MMC) have a different construction design and operating principles than PWM-driven converters. They comprise several small DC choppers with bi-directional switches, making up sub-modules of each leg of the three-phase converter. Assuming that the output DC voltage of each sub-module is controlled to maintain an average value of E_{dc} then the constant input DC voltage in each leg of a three-phase MMC-VSC with N sub-modules would be $E_{DC} = N \times E_{dc}$ [11]-[12]. It follows that the number of active sub-modules in the multi-level converter dictates the value of the voltage magnitude on the AC side of the converter. It turns out that (1) also represents very well the aggregated affects of this operation if one thinks of m_a as a discrete tap as opposed to the continuous tap associated with the PWM-driven VSC converters. For numerical efficiency within the power flow or the OPF solution a continuous tap is assumed and at the end of the convergent solution, the nearest physical tap is selected and one further iteration is carried out to fine tune the overall power flow solution. This would not be different to schemes adopted elsewhere for the tap selection of LTC transformers where discrete taps are considered as opposed to continuous ones [14].

As shown in Fig. 1 (b), the complex tap-changing transformer represents the internal operation of the converter under PWM control. The converter's input DC voltage, E_{DC} is provided by the capacitor bank $C_{DC,}$ which is connected in parallel with a resistor (conductance) of value G_{sw} representing the converter's internal switching losses at a constant DC input voltage. The reactive power control feature of the VSC is, on the other hand, represented in the valve set modeled by a notional variable shunt susceptance in the AC side of the ideal, complex, tap-changing transformer. The VSC model is completed by adding a series impedance to the AC side of the complex-tap transformer in which the series resistor R_1 is associated with the ohmic losses which are proportional to the AC terminal current squared and the series inductance X_1

represents the converter's interface magnetics.

The converter's switching losses are modeled by the following quadratic expression [1],

$$G_{sw} = G_0 \left(\frac{I_2^{act}}{I_2^{nom}} \right)^2 \tag{2}$$

where G_0 is the converter switching losses under constant DC voltage and nominal load current conditions. To incorporate the effects of actual converter operation this term is corrected by the squared ration of actual-to-nominal current – with the quadratic exponent chosen to reflect the power behavior of the switching resistance (conductance).

The reactive power property of the converter is modeled using a variable shunt branch susceptance to account for the calculated reactive power (either generation or absorption) in the converter depending on its control requirements, which may be set to either direct nodal voltage regulation or reactive power control [1].

The VSC's operation at fundamental frequency is defined by the following nodal admittance matrix which is developed in more detail in Appendix A:

$$\begin{pmatrix} \bar{I}_{vR} \\ \bar{I}_0 = 0 \end{pmatrix} = \begin{pmatrix} \bar{Y}_1 & -m_a'(\cos\varphi + \mathrm{j}\sin\varphi)\bar{Y}_1 \\ -m_a'(\cos\varphi - \mathrm{j}\sin\varphi)\bar{Y}_1 & m_a'^2(\bar{Y}_1 + jB_{eq}) + G_{sw} \end{pmatrix} \begin{pmatrix} \bar{V}_{vR} \\ V_0 \end{pmatrix} \tag{3}$$

Furthermore, the coupling transformer is taken to be a conventional tap-changing transformer with discrete tap steps, as shown in Fig. 1(c). The nodal matrix representation of the classical tap-changing transformer, represented by the equivalent circuit of Fig. 1(c), is [2]:

$$\begin{pmatrix} \bar{I}_k \\ \bar{I}_{vR} \end{pmatrix} = \begin{pmatrix} \bar{Y}_l & -T\bar{Y}_l \\ -T\bar{Y}_l & T^2\bar{Y}_l \end{pmatrix} \begin{pmatrix} \bar{V}_k \\ \bar{V}_{vR} \end{pmatrix} \tag{4}$$

Notice that in (4) the tap is real as opposed to complex and that it is taken to be on the transformer's primary side. It should be noted that in the course of the OPF solution process the OLTC tap is treated as a continuous variable but in practice this is a discrete variable. Therefore, at the end of each internal iterative loop, T is rounded off to its nearest integer.

A. STATCOM nodal power equations

The nodal power equations of the full STATCOM model within the OPF is calculated by combining the nodal power equations of the VSC and the OLTC modules.

1) VSC Module:

The VSC nodal power injections are derived from the product of its nodal voltages and current injections, in complex conjugate forms:

$$\begin{aligned} \begin{pmatrix} S_{vR}^{VSC} \\ S_0 \end{pmatrix} &= \begin{pmatrix} \bar{V}_{vR} & 0 \\ 0 & V_0 \end{pmatrix} \begin{pmatrix} I_{vR}^* \\ I_0^* \end{pmatrix} \\ &= \begin{pmatrix} \bar{V}_{vR} & 0 \\ 0 & V_0 \end{pmatrix} \left\{ \begin{pmatrix} \bar{Y}_1^* & -m_a'(\cos\varphi - \mathrm{j}\sin\varphi)\bar{Y}_1^* \\ -m_a'(\cos\varphi + \mathrm{j}\sin\varphi)\bar{Y}_1^* & m_a'^2(\bar{Y}_1^* - jB_{eq}) + G_{sw} \end{pmatrix} \begin{pmatrix} \bar{V}_{vR}^* \\ V_0 \end{pmatrix} \right\} \end{aligned} \tag{5}$$

Carrying out straightforward complex algebra, the nodal active and reactive power equations for the VSC model are derived:

$$\begin{aligned} P_{vR}^{VSC} &= G_1 V_{vR}^2 - m_a' V_{vR} V_0 \left[G_1 \cos(\theta_{vR} - \theta_0 - \phi) + B_1 \sin(\theta_{vR} - \theta_0 - \phi) \right] \\ Q_{vR}^{VSC} &= -B_1 V_{vR}^2 - m_a' V_{vR} V_0 \left[G_1 \sin(\theta_{vR} - \theta_0 - \phi) - B_1 \cos(\theta_{vR} - \theta_0 - \phi) \right] \\ P_0 &= \left(m_a'^2 G_1 + G_{sw} \right) V_0^2 - m_a' V_k V_0 \left[G_1 \cos(\theta_0 - \theta_{vR} + \phi) + B_1 \sin(\theta_0 - \theta_{vR} + \phi) \right] \\ Q_0 &= -\left(m_a'^2 (B_1 + B_{eq}) \right) V_0^2 - m_a' V_k V_0 \left[G_1 \sin(\theta_0 - \theta_{vR} + \phi) - B_1 \cos(\theta_0 - \theta_{vR} + \phi) \right] \end{aligned} \tag{6}$$

2) OLTC module:

Similarly, the nodal power injections of the OLTC module are derived from the nodal voltage and current relationships at both ends of the OLTC:

$$\begin{aligned} \begin{pmatrix} S_k^{OLTC} \\ S_{vR}^{OLTC} \end{pmatrix} &= \begin{pmatrix} \bar{V}_k & 0 \\ 0 & \bar{V}_{vR} \end{pmatrix} \begin{pmatrix} I_k^* \\ I_{vR}^* \end{pmatrix} \\ &= \begin{pmatrix} \bar{V}_k & 0 \\ 0 & \bar{V}_{vR} \end{pmatrix} \left\{ \begin{pmatrix} \bar{Y}_l^* & -T\bar{Y}_l^* \\ -T\bar{Y}_l^* & T^2\bar{Y}_l^* \end{pmatrix} \begin{pmatrix} \bar{V}_k^* \\ \bar{V}_{vR}^* \end{pmatrix} \right\} \end{aligned} \tag{7}$$

This expression yields the following explicit nodal power injections for the OLTC model:

$$\begin{aligned} P_k^{OLTC} &= G_l V_k^2 - T V_k V_{vR} \left[G_l \cos(\theta_k - \theta_{vR}) + B_l \sin(\theta_k - \theta_{vR}) \right] \\ Q_k^{OLTC} &= -B_l V_k^2 - T V_k V_{vR} \left[G_l \sin(\theta_k - \theta_{vR}) - B_l \cos(\theta_k - \theta_{vR}) \right] \\ P_{vR}^{OLTC} &= \left(T^2 G_l \right) V_{vR}^2 - T V_{vR} V_k \left[G_l \cos(\theta_{vR} - \theta_k) + B_l \sin(\theta_{vR} - \theta_k) \right] \\ Q_{vR}^{OLTC} &= -\left(T^2 B_l \right) V_{vR}^2 - T V_{vR} V_k \left[G_l \sin(\theta_{vR} - \theta_k) - B_l \cos(\theta_{vR} - \theta_k) \right] \end{aligned} \tag{8}$$

where $\bar{Y}_l = G_l + jB_l = 1/(R_l + jX_l)$.

Suitable combination of the two set of equations, (6) and (8), yields the required nodal power injections at the three nodes of interest, namely, *k*, *vR* and 0:

$$\begin{aligned} P_k^{cal} &= P_k^{OLTC} + \sum P_k \\ Q_k^{cal} &= Q_k^{OLTC} + \sum Q_k \end{aligned} \tag{9}$$

$$\begin{aligned} P_{vR}^{cal} &= P_{vR}^{VSC} + P_{vR}^{oltc} \\ Q_{vR}^{cal} &= Q_{vR}^{VSC} + Q_{vR}^{oltc} \end{aligned} \tag{10}$$

$$\begin{aligned} P_0^{cal} &= P_0 \\ Q_0^{cal} &= Q_0 \end{aligned} \tag{11}$$

where P_k and Q_k in the summation symbol in (9)-(10) are the contributions of all branches connected to node *k* other than the OLTC transformer. These calculated nodal powers are required by the Optimal Power Flow formulation.

B. Practical Implications

1) STATCOM Design Requirements:

As illustrated in Fig. 1(b), the VSC is assumed to be connected between a sending bus, *vR*, and a receiving bus, 0, with the former taken to be the VSC's AC bus and the latter taken to be the VSC's DC bus. The voltage input at the DC bus is provided by the DC capacitor bank, of value C_{DC}, and kept constant at a value E_{DC}. The voltage magnitude V_{vR} is regulated within system-dependent maximum and minimum

values afforded by the following basic relationships:

$$|V_{vR}| = m_a' E_{DC} + \sqrt{G_1^2 + B_1^2} \cdot |\bar{I}_1| \quad (12)$$

The PWM-controlled VSC is taken to operate within the linear region [6]. Hence, the PWM amplitude modulation coefficient is within the bounds: $0 < m_a < 1$ and for a two-level, three-phase VSC, $m_a' = \sqrt{3}/2 \cdot m_a$.

2) Simplifying assumptions:

It should be noted that the ideal phase shifter decouples, angle-wise, the circuits to the left and to the right of the ideal transformer, i.e., the phase angle value at node 0 is independent of circuit parameters or network complexity to the left of the ideal phase shifting transformer. From the numerical perspective, the phase angle voltage at bus 0 keeps its value given at the point of initialization, which in this STATCOM application will be taken to be zero - when looked at it from the vantage of rectangular coordinates, its imaginary part does not exist [1]. In the course of the OPF solution process the variations of the DC bus angle are kept to zero by penalizing this angle throughout the solution process, hence, $\Delta\theta_0 = 0$. Alternatively, the entries corresponding to this state variable in the OPF formulation may be removed altogether, resulting in a more compact formulation that would yield identical results.

III. STATCOM NEW MODEL FORMULATION IN OPTIMAL POWER FLOW (OPF) USING NEWTON'S METHOD

A. Augmented Lagrangian Functions

The constrained OPF problem is formulated using the Lagrangian function given in (13) for the STATCOM model by applying explicit multipliers to system equality constraints given in (9)-(11) and penalizing the resultant Lagrangian function for any state variable violations [2]:

$$L(x,\lambda,u) = F(P_G) + \lambda^t H(x) + P(x,u) \quad (13)$$

where *H(x)* corresponds to the set of functional equality constraints for the system including the STATCOM device. $F(P_G)$ corresponds to the summation of the values of the problem's objective functions which are taken to be the generators' quadratic cost functions as given in [13]. And, *P(x,u)* is an explicit quadratic penalty function for penalizing the Lagrangian function for any state variable violations.

The explicit state variables pertaining to the STATCOM new model comprise the variables for both the converter and the OLTC modules. This is shown in (14):

$$x_{STATCOM} = \left[\theta_k \quad \theta_{vR} \quad \theta_0 \quad V_k \quad V_{vR} \quad V_0 \quad m_a' \quad \phi \quad T\right]^T \quad (14)$$

It should be noted that apart from these explicit expressions, solving the OPF requires defining a Lagrangian function for the whole system which would include the nodal voltages and phase angles of all buses (except for the Slack bus for which only the nodal voltage magnitude is required), transformer tap ratios, as well as any other variables associated with a given power controlling equipment such as the STATCOM. As mentioned in Section I this is done by combining the effects of all the system Lagrangian functions.

The OPF problem to be solved in this paper is on the cost of generators' active power dispatch, each possessing a quadratic cost function with an expression similar to the one presented in [11].

P_G in (13) then corresponds to the generators' scheduled active power dispatch which is subject to the system's operating conditions (i.e. *H(x)*). In such circumstances the OPF problem is concerned with minimizing the overall cost of active power dispatch subject to realistic operational conditions and control settings. The controls are set by the STATCOM explicit state variables in the system. The problem constraints essentially represent the network actual operating conditions. Voltage magnitudes and phase angles in buses, generators' active powers, nodal power injections and mismatches in each bus are among the most important operating constraints in OPF-related studies. Applying Newton's method [15]-[18] to the Lagrangian function (13) and assuming that no penalty function terms exist at the start of the OPF iterative process – the system is assumed to work under normal operating conditions and all the variables are initialized within their respective limits – the linearized system of equations for the OPF is defined as:

$$\nabla_{zz}^2 L(z) \times \Delta z = -\nabla_z L \quad (15)$$

where vector $z = [x, \lambda, u]^T$ is the vector of primal-dual variables (dual variables are the Lagrange multipliers for both equality and inequality constraints, λ and *u*, respectively) [15]-[18].

The matrix of coefficients, $\nabla_{zz}^2 L(z)$, is a combination of *Hessian* and *Jacobian* terms obtained from second order derivatives of the Lagrangian function in (13) with respect to the entries of vector *z*. This results in a formulation which yields a quadratic rate of convergence. Commensurate with the power flow Newton-Raphson application, the Jacobian sub-matrix in (15) keeps the same level of sparsity as the nodal admittance matrix and so does its Hessian sub-matrix. This contrasts with an earlier formulation based solely on the use of an alternative Hessian matrix [20], which contains little sparsity. The *gradient vector*, $\nabla_z L$, which comprises the first order derivatives of the Lagrangian function with respect to the entries of vector *z* ought to maintain a decreasing pace throughout the course of the iterative solution [2], [18]-[20], to ensure a reliable solution towards the optimum.

The linearized system of equations may be written down more explicitly as:

$$\left[\begin{array}{cc:c} H_{xx} & H_{xy} & J_{x\lambda} \\ H_{yx} & H_{yy} & J_{y\lambda} \\ \hdashline J_{\lambda x} & J_{\lambda y} & 0 \end{array}\right] \times \begin{bmatrix} \Delta x \\ \Delta y \\ \Delta\lambda \end{bmatrix} = -\begin{bmatrix} g_x \\ g_y \\ g_\lambda \end{bmatrix} \quad (16)$$

It should be noted that the gradient term, g_λ, actually corresponds to the mismatch of nodal power calculations. It should also be noted that the second order derivatives of the Lagrangian function with respect to the Lagrange multipliers

are zero, i.e., $H_{\lambda\lambda} = \nabla^2_{\lambda\lambda} L(x,\lambda,y) = 0$.

B. STATCOM New Model Equality Constraints

For the STATCOM model in Fig. 1, the set of functional constraints comprise the nodal active and reactive power mismatch equations at nodes: *k*, *vR* and 0,

$$P_k^{cal} - P_{g_k} + P_{d_k} = 0 \quad (17)$$

$$Q_k^{cal} - Q_{g_k} + Q_{d_k} = 0 \quad (18)$$

$$P_{vR}^{cal} - P_{g_{vR}} + P_{d_{vR}} = 0 \quad (19)$$

$$Q_{vR}^{cal} - Q_{g_{vR}} + Q_{d_{vR}} = 0 \quad (20)$$

$$P_0^{cal} - P_{g_0} + P_{d_0} = 0 \quad (21)$$

$$Q_0^{cal} - Q_{g_0} + Q_{d_0} = 0 \quad (22)$$

where P_k^{calc} and Q_k^{calc} are the calculated injected powers at node *k*; P_{g_k} and Q_{g_k} are active and reactive powers generated at node *k*; P_{d_k} and Q_{d_k} are active and reactive powers consumed at node *k*; P_{vR}^{calc} and Q_{vR}^{calc} are the calculated injected powers at node *vR*; $P_{g_{vR}}$, Q_{gvR}, $P_{d_{vR}}$ and $Q_{d_{vR}}$ will be zero for any practical purpose; P_0^{calc} and Q_0^{calc} are the calculated injected powers at node 0; P_{g_0}, Q_{g0}, P_{d_0} and Q_{d_0} are the active and reactive power generated and consumed at node 0, respectively. The above expressions have to be satisfied for an optimum solution to be acceptable, otherwise it is said that the solution is infeasible.

C. STATCOM New Model Control in OPF

Two control modes are available in the STATCOM new model introduced in this paper, namely, active power flow control (if applicable) and nodal voltage regulation - *control constraints* given in (23) and (24) are used to this end.

1) Nodal Voltage Regulation - Constraint on State Variables

The voltage regulation constraint is a variable equality constraint which is added to the OPF formulation by means of a quadratic penalty function of the form (23) [12].

$$P_{V_i} = \frac{1}{2} S \cdot (V_i - V_i^{reg})^2 \quad (23)$$

where *i* is either *k* or 0 and V_i^{reg} is the target nodal voltage magnitude which must remain within operational limits and S is a non-zero integer termed the penalty factor.

Eq. (23) is used by default to enforce the STATCOM's nodal voltage regulation at the AC bus using the OLTC transformer in Fig. 1(c). It should be noted that within the OPF formulation, the nodal voltages at both nodes *k* (AC system voltage) and *vR* (VSC AC output voltage) may be controlled by the combined action of the OLTC and VSC. However, the VSC AC system voltage is rather set free to vary within its permitted boundaries; as a result of this, nodal voltage regulation is not imposed on this node. The VSC DC input voltage is provided by the DC capacitor bank which is initialized as a PV-type bus in the OPF solution process. The VSC explicit nodal voltage control is therefore on the DC bus not on the AC bus. The AC side voltage is regulated by the action of the OLTC transformer, whereas the DC side voltage is determined by the DC capacitor's design requirements - as discussed in Section II.B. Hence, the DC voltage is set to a pre-determined level (corresponding to the VSC input DC voltage) throughout the solution process.

The value of the penalty factor, *S*, dictates the hardness of the voltage regulation boundaries. However, choosing the initial value of the penalty factor is a highly empirical exercise, which is rooted in experience and trial and error [2]. Choosing too large a value may lead to inaccurate and unfeasible results whereas small values may lead to a poor rate of convergence and possible stagnation. For the test cases presented in this paper a value of 10^{10} has been used for the penalty factor *S*.

2) Active Power Flow Regulation – Constraint on Functions

Active power flow through the VSC converter is controlled by varying the phase shift that exists in the converter's ideal transformer model (i.e. the angle φ).

For explicit active power flow control inside the converter, an additional functional equality constraint is introduced in form of (24):

$$P_{conv} - P_{conv}^{spe} = 0 \quad (24)$$

where normally $P_{conv} = P_0^{calc}$ is the calculated nodal active power at the DC bus, which is set to zero or $\pm P_{dc}$, as detailed above. For the purposes of modeling the VSC's DC bus, this is a PV-type bus with active power set to either zero or to a pre-specified value, say, $\pm P_{dc}$.

Notice that the latter option is only possible if any form of energy storage is available in the STATCOM's DC bus. However, reactive power in the DC node is always set to zero. In contrast to the model of the VSC based on the concept of a controllable voltage source, in the new STATCOM model the OPF algorithm modifies the phase angle φ in such a way that the amount of the active power flowing through the converter corresponds to the target active power flow upon convergence. This is a distinguished feature of the new model which is completely absent from the controllable voltage source model. The explicit Jacobian and Hessian terms associated with the active power flow control constraint in the STATCOM model are given in Appendix B.

D. STATCOM's explicit Lagrangian function

The STATCOM's Lagrangian function is given by (25).

$$\begin{aligned} L_{STATCOM} &= \lambda_{p_k}(P_k^{calc} + P_{g_k} - P_{d_k}) + \lambda_{q_k}(Q_k^{calc} + Q_{g_k} - Q_{d_k}) \\ &+ \lambda_{p_{vR}}(P_{vR}^{calc} + P_{g_{vR}} - P_{d_{vR}}) + \lambda_{q_{vR}}(Q_{vR}^{calc} + Q_{g_{vR}} - Q_{d_{vR}}) \\ &+ \lambda_{p_0}(P_0^{calc} + P_{g_0} - P_{d_0}) + \lambda_{q_0}(Q_0^{calc} + Q_{g_0} - Q_{d_0}) \\ &+ \lambda_{\varphi}(P_{conv} - P_{conv}^{spec}) \end{aligned} \quad (25)$$

The Lagrangian in (25) contains no quadratic penalty function for inequality constraints at the start of the OPF process, i.e. these are not activated at the outset. A full iterative solution of (15) requires the convergence of an inner loop by solving (16) in a true Newton-Raphson fashion. Once the process converges to a specified tolerance in the inner loop then all the variable limits are checked against their respective boundaries and the active binding set is identified [17]-[18]. Variables that have violated their limits make up the active set; they are forced to their ceilings and incorporated in (15) using the penalty function *P(x,u)* in which the term *u* is defined as the Lagrangian multiplier for its corresponding active set. Inclusion of the active set upon convergence of the first inner loop completes the first iteration of the outer loop – referred to as a one global iteration. Hence, a second outer loop is initiated, which now incorporates both equality and inequality constraints [15], [18], and [21]-[22]. In principle, convergence for the local iterations is achieved in true quadratic fashion – a hall-mark of the Newton-Raphson method. However, the active set is updated outside the Newton-Raphson solution, a procedure that impairs the overall convergence of the Newton-Raphson OPF solution, which is termed Newton's OPF method. Furthermore, experience has shown that the inner loops' convergence may be better assured by employing a decelerating factor ($0<\alpha<1$) at the point of updating the state variables and Lagrange multipliers at the end of each local iteration. This is particularly the case during the local iterations of the first two global iterations [2]. The use of such deceleration factors impairs further the quadratic convergence characteristics of the Newton-Raphson method, i.e., the number of local iterations will increase. However, experience has shown that this is a very powerful resource owing to the highly non-linear nature of the problem at hand.

The active power flow constrain at the converter, (23), is normally enforced by default at the start of the solution process – its Lagrangian is included in (25). It is either set to zero DC power or to a pre-specified DC positive/negative power injection if the STATCOM is provided with any form of energy storage. Of course, it is always possible in Newton's OPF solution not to wish to enforce this constrain, something that is done by enforcing its associated Lagrange multiplier to zero using a suitable quadratic penalty function of the form given in (26).

$$P_{\lambda_\phi} = \frac{1}{2} S \lambda_\phi^2 \tag{26}$$

where the term λ_ϕ is the Lagrangian multiplier pertaining to the converter's active power flow constraint. It is noted that all the multipliers in (25) have been initialized at zero values.

E. STATCOM linearized system of equations

Application of Newton's method to the STATCOM Lagrangian function (25), taking due account of the state variable vector (15) and the Lagrange multipliers for the active equality constraints set, is given in (27).

$$\begin{bmatrix} \partial^2 L/\partial\theta^2 & \partial^2 L/\partial\theta\,\partial V & \partial^2 L/\partial\theta\,\partial m_a' & \partial^2 L/\partial\theta\,\partial\phi & \partial^2 L/\partial\theta\,\partial T \\ \partial^2 L/\partial V\,\partial\theta & \partial^2 L/\partial V^2 & \partial^2 L/\partial V\,\partial m_a' & \partial^2 L/\partial V\,\partial\phi & \partial^2 L/\partial V\,\partial T \\ \partial^2 L/\partial m_a'\partial\theta & \partial^2 L/\partial m_a'\partial V & \partial^2 L/\partial m_a'^2 & \partial^2 L/\partial m_a'\partial\phi & \partial^2 L/\partial m_a'\partial T \\ \partial^2 L/\partial\phi\partial\theta & \partial^2 L/\partial\phi\,\partial V & \partial^2 L/\partial\phi\,\partial m_a' & \partial^2 L/\partial\phi^2 & \partial^2 L/\partial\phi\,\partial T \\ \partial^2 L/\partial T\partial\theta & \partial^2 L/\partial T\partial V & \partial^2 L/\partial T\,\partial m_a' & \partial^2 L/\partial T\,\partial\phi & \partial^2 L/\partial T^2 \\ \partial P^{calc}/\partial\theta & \partial P^{calc}/\partial V & \partial P^{calc}/\partial m_a' & \partial P^{calc}/\partial\phi & \partial P^{calc}/\partial T \\ \partial Q^{calc}/\partial\theta & \partial Q^{calc}/\partial V & \partial Q^{calc}/\partial m_a' & \partial Q^{calc}/\partial\phi & \partial Q^{calc}/\partial T \\ \partial P_{conv}/\partial\theta & \partial P_{conv}/\partial V & \partial P_{conv}/\partial m_a' & \partial P_{conv}/\partial\phi & \partial P_{conv}/\partial T \end{bmatrix} \begin{bmatrix} \partial P^{calc}/\partial\theta & \partial Q^{calc}/\partial\theta & \partial P_{conv}/\partial\theta \\ \partial P^{calc}/\partial V & \partial Q^{calc}/\partial V & \partial P_{conv}/\partial V \\ \partial P^{calc}/\partial m_a' & \partial Q^{calc}/\partial m_a' & \partial P_{conv}/\partial m_a' \\ \partial P^{calc}/\partial\phi & \partial Q^{calc}/\partial\phi & \partial P_{conv}/\partial\phi \\ \partial P^{calc}/\partial T & \partial Q^{calc}/\partial T & \partial P_{conv}/\partial T \\ 0 & 0 & 0 \\ 0 & 0 & 0 \\ 0 & 0 & 0 \end{bmatrix} \begin{bmatrix} \Delta\theta \\ \Delta V \\ \Delta m_a' \\ \Delta\phi \\ \Delta T \\ \Delta\lambda_p \\ \Delta\lambda_q \\ \Delta\lambda_\phi \end{bmatrix} = - \begin{bmatrix} \nabla_\theta L \\ \nabla_V L \\ \nabla_{m_a'} L \\ \nabla_\phi L \\ \nabla_T L \\ \Delta P^{calc} \\ \Delta Q^{calc} \\ P_{conv} - P_{conv}^{spec} \end{bmatrix} \tag{27}$$

F. The inequality constraints set

The inequality constraint set includes the following limits: the converter's PWM amplitude modulation coefficient, m_a', the OLTC transformer's tap ratio, *T*, and the nodal voltage magnitudes. The control variables are the STATCOM's nodal voltages at both nodes (AC and DC), the ideal transformer's complex tap, $m_a'\angle\phi$, which is allowed to vary between 0 and $\sqrt{3}/2$ and the OLTC's tap ratio, *T* which is allowed to vary between 0.6 and 1.2. No limits are imposed in the phase angles of the nodal voltages or in the VSC's complex tap angle.

IV. Test Cases

To assess the accuracy, flexibility and robustness of the proposed STATCOM model, two test cases are presented in this section. The first case is a rather contrived system where the STATCOM is fed from a synchronous generator through a transmission line, as shown in Fig. 2. The second case comprises a modified version of the IEEE 30-node system [23] in which a STATCOM is assumed connected at node 24 to maintain voltage magnitude at 1 p.u. at that node. An existing OPF program using Newton's method written in MATLAB© [2] has been extended to implement the new STATCOM model and to carry out quite comprehensive tests, two of which are presented below.

A. Radial System – New Model

The three-node system in Fig. 2 comprises one generator, one transmission line, one load and one STATCOM which is used to regulate voltage magnitude at its AC node at 1.02 p.u. whereas its DC bus voltage is kept at $\sqrt{2}$ p.u.. The following parameters are used in the contrived test system - (i)

transmission line: R_{LT}=0.05 p.u. and X_{LT}=0.10 p.u.; (ii) LTC transformer: R_{TR}=0.01 and X_{TR}=0.10 p.u.; (iii) VSC: R_{VSC}=0.01 p.u., X_{VSC}=0.10 p.u., G_0=0.0100 and B_{eq}=0.50 p.u.; (iv) Load: P_L=0.25 p.u. and Q_L=0.20 p.u.

The generator node is taken to be the slack bus. The objective function to be minimized is shown below:

$$f(P_G) = 60 + 3.4P_G + 0.004P_G \quad (28)$$

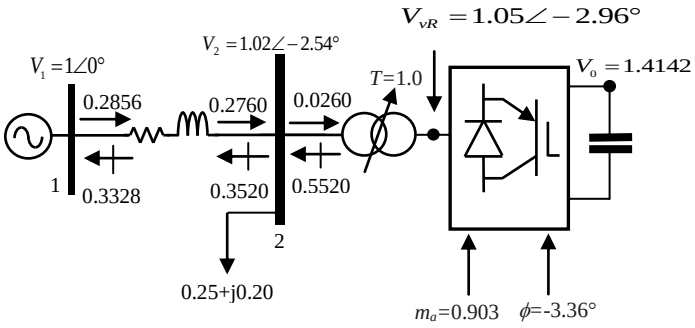

Fig. 2: Fictitious three-node Radial System – STATCOM New Model Representation

The optimal power flow solution for the radial system is given in table I. The voltage at the slack bus is also penalized to keep it at 1 p.u.. The VSC DC voltage is fixed at 1.4142 p.u. and the voltage at bus 2 is controlled using the LTC transformer. The final value of the variable tap changer at the optimum is 1.02 which is rounded off to 1.0 for a discrete mechanical tap. The nodes *STATCOM-AC* and *STATCOM-DC* in table I, correspond to the AC and DC nodes of the STATCOM, respectively; *Gen* corresponds to the generator bus; and *VSC-AC* and *VSC-DC* correspond to the AC and DC nodes of the Voltage Source Converter as given by the new model shown in Fig.1. The final value of the objective function in (28) is calculated according to the generator's optimum active power dispatch, with values given in table II. The values of the penalty factors *S* for all the quadratic penalty functions are initiated at 10^{10}.

The OPF for the radial system in Fig. 2 converges in three global iterations to a tolerance of 10^{-9}. Table III gives the number of local iterations incurred at each global iteration, with a deceleration factor α=0.025. The converter's AC terminal voltage is free to vary within its allowable boundaries and arrives at the final value of 1.05 p.u. with the angle of -2.96. The voltage angle at the DC bus is kept constant at the point of initialization using a quadratic penalty function to nullify its corresponding increments throughout the OPF process. The STATCOM consumes 0.0260 p.u of active power and the converter switching losses are G_{sw}=0.59%.

The converter valve set generates 0.6120 p.u. of reactive power to maintain the voltage at bus 2 at 1.02 p.u. Furthermore, minimum transmission line losses stand at P_{loss}=0.0096 p.u. and Q_{loss}=0.0192 p.u. The generator's active and reactive powers limits are set at: $0.1 \le P_{gen} \le 2$ and $-5 \le Q_{gen} \le 5$ p. u. respectively.

TABLE I
OPTIMAL POWER FLOW SOLUTION FOR THE FICTITIOUS RADIAL THREE-NODE SYSTEM – NEW MODEL

Bus	Active Power (p.u.)	Reactive Power (p.u.)
Gen	0.2856	-0.3328
STATCOM-AC	-0.0260	0.5520
STATCOM-DC	0.00	0.00
VSC-AC	0.0231	-0.5814

TABLE II
OBJECTIVE FUNCTION VALUE AT THE OPTIMUM

Generator	Objective Function Value
1	160.3726 $/hr

TABLE III
GLOBAL ITERATIONS AND LOCAL ITERATIONS

Global	Local
1	20
2	15
3	7

B. Radial System – Controllable Voltage Source Model

For the sake of completeness and in order to contrast the results provided by the new model with those provided by the STATCOM model based on the controllable voltage source concept [2]–[3], the contrived radial system of Fig. 2 is solved again but this time using the latter model. The voltage source is connected behind a coupling impedance (representing the VSC internal magnetic and ohmic losses). A shunt conductance of value 1% is connected between the coupling impedance and the voltage source in order to represent the ohmic losses inside the converter.

The three-node system with the STATCOM modeled as a controllable voltage source is shown in Fig. 3.

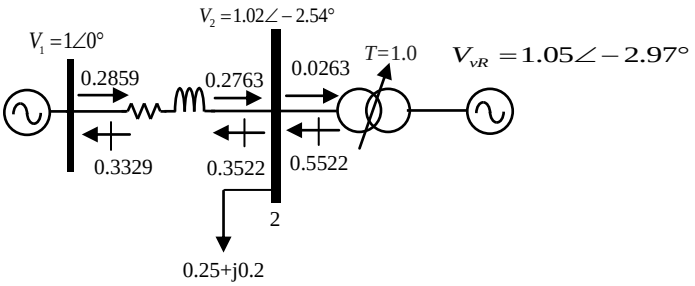

Figure 3 – Fictitious Three-node Radial System – STATCOM Controllable Voltage Source Model Representation

The network parameters for this system remain very much the same as in the test case of Fig. 2. The OPF solution converges in 3 global iterations. These results are compared to those produced by the new STATCOM model in tables IV-V. As expected both models yield similar results. The STATCOM controllable voltage source model generates 0.6110 p.u. of reactive power to maintain the voltage at node 2 at 1.02 p.u.

The converter voltage (V_{vR}) stands at 1.0510 p.u. The converter voltages behind the converter impedance for both models are compared in tables IV-V.

TABLE IV
CONVERTER VOLTAGE MAGNITUDES FOR DIFFERENT STATCOM MODELS

Voltage Magnitude	New Model	Controllable Voltage Source Model
V_{conv}	1.1062	1.1062
V_2	1.02	1.02

TABLE V
CALCULATED VOLTAGE PHASE ANGLES FOR DIFFERENT STATCOM MODELS

Voltage Phase Angle	New Model	Controllable Voltage Source Model
Φ	-3.360	-3.358
θ_2	-2.96	-2.96

The powers calculated by both models are presented in table VI. The switching losses in this test case are modeled by connecting a shunt conductance of 1% between the coupling impedance and the variable voltage source. In fact, this shunt resistive branch should be connected at the DC bus of the VSC as opposed to its AC side but is precluded because the voltage source converter model does not have such a bus and the results concerning switching losses will be inaccurate and optimistic.

TABLE VI
OPTIMAL POWER FLOW SOLUTION FOR DIFFERENT STATCOM MODELS

New Model	Active Power (p.u.)	Reactive Power (p.u.)
Gen	0.2856	-0.3328
STATCOM-AC	-0.0260	0.5520
STATCOM-DC	0.00	0.00
Controllable Voltage Source	**Active Power (p.u.)**	**Reactive Power (p.u.)**
Gen	0.2859	-0.3329
STATCOM-AC	-0.0263	0.5522
STATCOM-DC	N/A	N/A

By comparing the results given by the OPF solution of the three-node radial system with the STATCOM modeled using the new model and a controllable voltage source model respectively, the following limitations are clearly observed, (i) lack of explicit DC bus representation which means that the converter voltage is represented by only one state variable pertaining to the controllable voltage source. Therefore there is no direct means of controlling the AC output voltage of the converter by varying the DC input voltage. (ii) In the controllable voltage source model there is no way of limiting the operation of the PWM modulation coefficient within the linear region, therefore the results obtained from a controllable voltage source model do not provide sufficient information to distinguish the regions of operation of the converter. This may be done by only introducing a new explicit state variable in the OPF formulation, further complicating the overall formulation of the problem, whereas, with the new model, this is already included in form of the complex tap ratio of the transformer modeling the PWM-control of the VSC. (iii) Lack of the capability of appropriate modeling of energy storage in the DC side of the converter due to the inability for explicit representation of the DC-side bus. This may be remedied by adding an additional equality constraint in form of an active power flow, however with the new model; this is included inherently within the converter model. All is needed to add the energy storage is to change the value of the converter active power flow control to a non-zero negative value. (iv) Inaccurate and optimistic calculation of the converter's internal switching losses.

Carrying out the OPF solution with this a priori detected modeling inaccuracy will yield a different optimum operating point (i.e. 157.07 $/hr), which is optimistic.

C. Modified IEEE 30-node System

In order to test the performance of the new STATCOM model in a larger network, the IEEE 30-node system [23] is selected. The fixed bank of capacitors at node 24 is replaced with a STATCOM, which is used to regulate voltage magnitude at that node at 1.02 p.u.. The modified portion of the 30-node system is shown in Fig. 4. The nodal voltage magnitudes are allowed to vary between 0.9 and 1.1 p.u. at all 24 load buses and between 0.9 and 1.05 p.u. at all six generator buses. Node 1 is taken to be the slack bus.

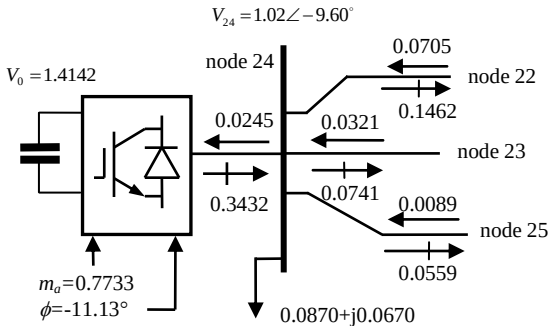

Fig. 4: STATCOM supplying reactive power at node 24 of the modified IEEE 30-node system to regulate voltage magnitude at 1.02 p.u.

All the STATCOM parameters and limits are taken to be the same as in Test Case A except for the transformer leakage reactance, which takes a value of 0.3690 p.u. (the tap changing transformer is not shown in Fig. 4). The penalty factor *S* for each quadratic penalty function is initiated at 10^{10}.

The generators' fuel cost functions given in Table VII are used for the six generators available in the 30-node test system.

The Newton's OPF arrives to the solution in eight global iterations. The slow convergence rate is the result of enforcing inequality constraints in voltage magnitudes for violated nodes. A summary of the most relevant results are shown in tables VIII-X. The STATCOM consumes 0.0245 p.u. of active power of which 0.81% is for VSC internal switching losses, whilst 1.64% accounts for OLTC ohmic losses. The STATCOM generates 0.3432 p.u. of reactive power to maintain the voltage magnitude at node *24* to 1.02 p.u. The OLTC final tap is rounded off to 0.7. Notice that the powers

shown are the output powers at the OLTC transformer terminals as opposed to the VSC terminals. Table X shows the final values of generator cost functions at the optimum after eight global iterations to a tolerance of 10^{-9}. The increased number of iterations was due to a voltage limit violation in node 24 which has been fixed to its lower boundary by the action of its inequality constraint multiplier. The total value of the objective function is the sum of all six generators' costs obtained with the generators' outputs at the optimum, which stands at 972.8759 $/hr.

TABLE VII
FUEL COST FUNCTIONS OF THE SIX GENERATORS IN THE IEEE 30-NODE TEST SYSTEM

Generator	Objective Function
1	$2P_{G_1} + 0.02P_{G_1}^2$
2	$1.75P_{G_1} + 0.0175P_{G_1}^2$
3	$1P_{G_1} + 0.0625P_{G_1}^2$
4	$3.25P_{G_1} + 0.083P_{G_1}^2$
5	$3P_{G_1} + 0.025P_{G_1}^2$
6	$3P_{G_1} + 0.025P_{G_1}^2$

TABLE VIII
ACTIVE AND REACTIVE POWER INJECTIONS AT THE GENERATOR AND STATCOM NODES

Bus	Active Power (p.u.)	Reactive Power (p.u.)
Gen 1_ node 1	0.5784	-0.1268
Gen 2_ node 2	0.7490	0.1230
Gen 3_node 5	0.2894	0.2660
Gen 4_node 8	0.7095	0.3797
Gen 5_node 11	0.2935	-0.2209
Gen 6_node 13	0.2837	0.2140
STAT_AC	-0.0245	0.3432
STAT_DC	0	0

TABLE IX
CONVERTER OPERATING PARAMETERS AT THE OPTIMUM

m_a	ϕ
0.7733	-11.13°

TABLE X
OBJECTIVE FUNCTIONS VALUES AT THE OPTIMUM

Generator	Objective Function Value
1	182.5997 $/hr
2	229.2370 $/hr
3	81.26670 $/hr
4	272.3566 $/hr
5	109.5990 $/hr
6	105.2440 $/hr

V. CONVERTER SWITCHING LOSSES

One of the advantages of the proposed new model is that it gives provisions for explicit representation of the converter's internal switching losses under converter's operating conditions. This is done by applying (2) to the converter's otherwise constant switching losses under constant input DC voltage and rated current (i.e. 1 p.u).

It is observed that applying the OPF formulation as outlined in this paper will result in a further reduction of the converter's switching losses even under similar operating conditions as for when a conventional power flow (CPF) algorithm is applied to the same model. This is evident in table XI when the new model is used in a fictitious three-node system similar to the one shown in Fig. 1 and the STATCOM is tasked with maintaining the voltage at node 2 to 1.05 p.u.

It is seen that applying the OPF under the same operating criteria will result in an approximate 30% reduction in the value calculated for the converter's switching losses. The STATCOM current magnitude in the case of OPF solution algorithm is 0.7095 p.u. whereas in the case of applying CPF the STATCOM current magnitude comes at 0.8421 p.u.

TABLE XI
SWITCHING LOSSES AS GIVEN BY OPF AND CPF SOLUTIONS – FICTITIOUS THREE-NODE SYSTEM

Solution Algorithm	STATCOM Switching Loss (%) – New Model
OPF	1.0068
CPF	1.42

VI. CONCLUSIONS

A new STATCOM model suitable for optimal power flow solutions using Newton's method has been introduced in this paper. The new model departs from the idealized controllable voltage source concept that has been used so far for representing the fundamental frequency operation of the STATCOM in OPF formulations. Instead, it treats the DC-to-AC converter of the STATCOM as a transformer device with a variable complex tap – just as DC-to-DC converters have been linked, conceptually speaking, to step-up and step-down transformers [6]. The PWM control of the VSC is modeled explicitly by means of the complex tap of the ideal transformer whose magnitude represents the PWM amplitude modulation coefficient and its phase angle corresponds to the phase shift that would exist between the fundamental frequency voltage and current wave forms. Moreover, the phase angle of the complex tap in the new VSC model coincides with the phase angle of the conventional, equivalent voltage source model of the VSC. The converter's DC bus is modeled as a type-PV bus with constant DC voltage magnitude and zero phase angle, i.e., when expressed in rectangular coordinates, the imaginary part of this voltage does not exist. The STATCOM-OPF model is tested in a radial system configuration to showcase the regulating properties of the new model. A larger system comprising several generators has been selected to show that the new STATCOM model performs equally well within Newton's

OPF solution.

APPENDIX A: VSC MODEL DESCRIPTION

The VSC is modeled as an ideal complex tap-changing transformer, as shown in Fig. 1(b). The following relationship defines the complex tap ratio in the ideal complex tap-changing transformer:

$$\frac{\bar{V}_1}{V_0} = \frac{m_a^{'}\angle\varphi}{1} \quad \& \quad \frac{m_a^{'}\angle-\varphi}{1} = \frac{\bar{I}_2}{\bar{I}_1 - \bar{I}_1'} \tag{A.1}$$

The nodal matrix equation is quite straightforwardly derived by performing basic nodal analysis on the VSC's equivalent circuit model in Fig. 1 (b). The current through the admittance connected to nodes *vR* and *1* is defined as:

$$\bar{I}_1 = \bar{Y}_1\left(\bar{V}_{vR} - \bar{V}_1\right) = \bar{Y}_1\bar{V}_{vR} - m_a^{'}\angle\phi\,\bar{Y}_1 V_0 = \bar{I}_{vR} \tag{A.2}$$

where $\bar{Y}_1 = 1/(R_1 + jX_1)$.

At node 0 the following relationship applies to the current flowing in this node:

$$\begin{aligned}\bar{I}_0 &= -\bar{I}_2 + \bar{I}_2' = m_a^{'}\angle-\varphi(\bar{I}_1 - \bar{I}_1') + G_{sw}\bar{V}_0 = \\ &= (-m_a^{'}\angle-\varphi)\bar{Y}_1\bar{V}_{vR} + (m_a^{'2}(\bar{Y}_1 + jB_{eq}) + G_{sw})\bar{V}_0\end{aligned} \tag{A.3}$$

Combining (A.2) and (A.3) will ultimately yield the VSC's nodal admittance matrix shown in (3).

APPENDIX B: EXPLICIT JACOBIAN AND HESSIAN TERMS FOR ACTIVE POWER FLOW REGULATION

In order to enforce the active power flow control capability of the VSC in the OPF solution a new explicit Lagrangian function may be defined as below:

$$L_\varphi = \lambda_\varphi(P_{conv} - P_{conv}^{spe}) \tag{B.1}$$

In which P_{conv} is the amount of VSC active power exchange with the grid and P_{conv}^{spe} is the specified target active power flow in the converter. The Hessian terms with respect to state variable *x* is given in (B.2) below:

$$\frac{\partial^2 L_\varphi}{\partial x\partial\lambda_\varphi} = \frac{\partial^2 L_\varphi}{\partial\lambda_\varphi\partial x} = \frac{dP_{conv}}{dx} \tag{B.2}$$

It is noted that normally P_{conv} corresponds to the DC side bus active power flow which is under normal circumstances set to zero unless an energy storage device is present in which case it is set to a pre-specified target value. The contribution of additional energy storage device will be extensively discussed in Appendix C.

The Hessian terms of (B.1) with respect to Lagrange multipliers are obviously zero, hence:

$$\frac{\partial^2 L_\varphi}{\partial\lambda_h\partial\lambda_\varphi} = \frac{\partial^2 L_\varphi}{\partial\lambda_\varphi\partial\lambda_h} = 0 \tag{B.3}$$

APPENDIX C: EFFECTS OF ENERGY STORAGE

The simplest of possible energy storage representations within the OPF formulation is done by applying an active power flow constraint in the converter and setting a target value for the DC power. The fictitious three-node system introduced in Fig. 2 is modified to include a small bank of batteries which inject 0.05 p.u. of active power into the system. The effects that the additional storage has in reducing the final value of the objective function are evident from table C.I. The final values of the converter's operational parameters are presented in table C.II. In this case the converter has a wider phase shift to allow for a larger active power flow from the converter to the grid.

TABLE C.I
EFFECTS OF ENERGY STORAGE ADDITION IN THE FICTITIOUS THREE-NODE RADIAL SYSTEM

Energy Storage (p.u.)	Slack Bus Active Power (p.u.)	Objective Function Final Value
N/A	0.2856	160.3726 $/hr
0.05	0.2330	141.4088 $/hr

TABLE C.II
CONVERTER PWM OPERATIONAL PARAMETERS AT OPTIMUM

Energy Storage (p.u.)	Final Tap Changer Magnitude (p.u.)	Phase Shift (deg)
N/A	0.9032	-3.36
0.05	0.8790	-2.47

APPENDIX D: THE IDEAL PHASE SHIFTER CIRCUIT

One salient characteristic of the new VSC model is that no special provisions within a conventional AC power flow solution algorithm is required to represent the DC circuit, since the complex tap-changing transformer of the VSC may be used with ease to give rise to the customary AC circuit and a notional DC circuit. However, some further explanation is required since the modelling development involves the conflation of AC and DC circuit concepts at an equivalent node, brought about by the use of the ideal tap-changing transformer concept.

In order to elaborate the explanation from the vantage of electronic circuits, we are going to assume that the conductance associated with switching losses, G_{sw}, in Fig. 1(b), may be referred to the primary side of the ideal transformer. The relevant part of the circuit illustrating such a situation but with capacitor representation, as opposed to its equivalent battery representation, is shown in Fig. D.1,

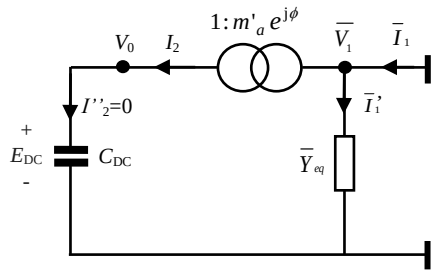

Figure D.1: Equivalent circuit showing the ideal phase-shifting transformer of Fig. 1(b) and neighboring elements, where $\bar{Y}_{eq} = G_{sw} + jB_{eq}$.

By invoking (A.1),

$$I_2 = m'_a e^{j\phi}(\bar{I}_1 - \bar{I}'_1) = I''_2 = 0 \quad \text{(D.1)}$$

$$V_0 = \frac{V_1}{m'_a e^{j\phi}} = \frac{V_1 e^{j\phi}}{m'_a e^{j\phi}} = \frac{V_1}{m'_a} = E_{DC} \quad \text{(D.2)}$$

In steady-state, a charged DC capacitor draws zero current and it is well-accepted that it may be represented as a charged battery [24] and, by extension, as a DC voltage source feeding no current. These facts are reflected by (D.1) and (D.2) and give the opportunity to interpret the circuit in Fig. D.1 in terms of electronic circuits concepts. Hence, it may be argued that in steady-state this circuit behaves as a nullor operating on a DC source representing the DC capacitor. The nullor is made up of a nullator and a norator [25], represented in this case by the ideal phase-shifting transformer and the equivalent admittance, $\bar{Y}_{eq}$, respectively. The circuit in Fig. D.1 may be re-drawn as follows,

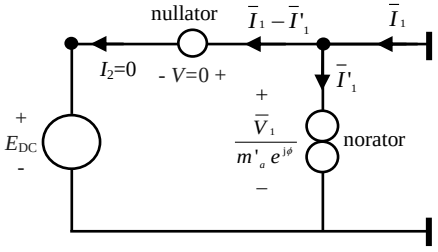

Figure D.2: Interpretation of the equivalent circuit of Fig. A.1 in terms of electronic circuit elements

The nullator and the norator are said to be *linear*, *time-invariant* one-port elements. The former is defined as having zero *current* through it and zero *voltage* across it. The latter, on the other hand, can have an arbitrary *current* through it and an arbitrary *voltage* across its terminals. Nullators have properties of both *short*-circuit (zero voltage) and *open-circuit* (zero current) connections. They are current and voltage sources at the same time. A norator is a voltage or *current source* with infinite gain. It takes whatever current and voltage is required by the external circuit to meet Kirchhoff's circuit laws. A norator is always paired with a nulator [25].

Either, by careful examination of (D.1) and (D.2) or by analysis of the electronic equivalent circuit in Fig. D.2, it can be seen that the ideal, complex tap-changing transformer of the VSC gives raise to the customary AC circuit and a notional DC circuit where the DC capacitor yields voltage E_{DC} but draws no current.

In a more general sense and from the viewpoint of the AC power flow solution, if resistive elements or DC power loads are connected to the notional DC bus then currents do pass through the ideal phase-shifting transformer but it would be a component of current that yields a nodal voltage V_0 with zero phase angle and, as one would expect, yields power with no imaginary component, hence, no reactive power exists in this part of the notional DC circuit.

VII. References

[1] E. Acha, and B. Kazemtabrizi "A New STATCOM Model for Power Flows Using the Newton-Raphson Method", *IEEE Trans. Power Systems*, Vol. 28, no.3, pp. 2455-2465

[2] E. Acha, C.R. Fuerte-Esquivel, H. Ambriz-Perez and C. Angeles-Camacho, *FACTS modeling and simulation in power networks.* John Wiley & Sons, 2005.

[3] G.N. Hingorani and L. Gyugyi, *Understanding FACTS: concepts and technologies of flexible ac transmission systems.* IEEE 2000.

[4] E. Acha, V. Agelidis, O. Anya-Lara and T.J.E., Miller, *Power Electronic Control in Electrical Systems*, Newnes Press, 2002.

[5] Y. Zhang, G. P. Adam, T.C. Lim, S.J. Finney, and B.W. Williams, "Voltage source converter in high voltage applications: multilevel versus two-level converters", presented at Ninth International Conference on AC and DC Power Transmission, (Conf. Publ. No. 0995), pp. 1-5, 19-21 Oct 2010

[6] N. Mohan, T.M. Undeland and W.P. Robins, *Power Electronics: Converters, Applications and Design*. John Wiley & Sons, 2003.

[7] L. Gyugi, "Dynamic compensation of AC transmission lines by solid-state synchronous voltage sources", *IEEE Trans. Power Delivery*, vol.9, no.2, pp. 904-911, April 1994

[8] D. J. Gotham and G. T. Heydt, "Power flow control and power flow studies for systems with FACTS devices", *IEEE Trans. Power Systems*, vol. 13, pp. 60-65, Feb. 1998

[9] X. Zhang and E. J. Handshcin, "Optimal power flow control by converter based FACTS controllers", presented at Seventh International Conference on the AC-DC Power Transmission, (Conf. Publ. No. 485), pp. 250-255, 28-30 Nov. 2001

[10] C. Angeles-Camacho, O. L. Tortelli, E. Acha and C. R. Fuerte-Esquivel, "Inclusion of a high voltage dc-voltage source converter model in a Newton-Raphson power flow algorithm", in *IEE Proc. Generation, Transmission and Distribution*, vol. 150, pp. 691-696, Nov. 2003

[11] A. Lesnicar, and R. Marquardt, "An innovative modular multilevel converter topology suitable for a wide power range", in *IEEE Proc. Power Tech Conference*, vol. 3, pp. 6-9, June. 2003

[12] M. Hagiwara, and H. Akagi, "PWM control and experiment of modular multilevel converters", presented at IEEE Power Electronics Specialists Conference, PESC 2008, pp.154-161, June 2008

[13] W. D. Stevenson and J. Grainger, *Power System Analysis.* Mc-Graw Hill 1994, pp. 531-587

[14] R. Garcia-Valle and E. Acha, "The incorporation of a discrete, dynamic LTC transformer model in a dynamic power flow algorithm", published in the proceedings of IASTED/Acta Press, Palma de Mallorca, Spain, May 2007

[15] D. P. Bertsekas, *Constrained Optimization and Lagrangian Multiplier Methods*, Academic Press, 1982

[16] G. Allaire, *Numerical Analysis and Optimization: An Introduction to Mathematical Modeling and Numerical Simulation.* Oxford University Press, 2007, pp. 306-388

[17] A. Ruszczynski, *Nonlinear Optimization*, Princeton University Press, 2005, pp. 286-331

[18] D. I. Sun, B Ashley, B. Brewer, A. Hughes and W. F. Tinney, "Optimal power flow by Newton's approach", *IEEE Trans. Power Apparatus and Systems*, vol. PAS-103, pp. 2864-2875, 1984

[19] H. W. Dommel and W. F. Tinney, "Optimal power flow solutions", *IEEE Trans. Power Apparatus and Systems,* vol. PAS-87, pp. 1866-1876, Oct. 1968
[20] A. M. Sasson, F. Viloria and F. Aboytes, "Optimal load flow solution using the Hessian matrix", *IEEE Trans. Power Apparatus and Systems*, vol. PAS-92, pp. 31-41, Jan. 1973
[21] A. Santos Jr. and G. R. M. da Costa, "Optimal power flow solutions by Newton's method applied to an augmented Lagrangian function", in *IEE Proc. Generation, Transmission and Distribution,* vol. 142, pp. 33-36, 1995
[22] A. Santos Jr., S. Deckmann and S. Soares, "A dual augmented Lagrangian approach for optimal power flow", *IEEE Trans. Power Systems,* vol. 3, pp. 1020-1025, Aug. 1998
[23] IEEE 30-node Test System. Available: http://www.ee.washington.edu/research/pstca
[24] J.W. Nilsson and S. Riedel, *Electric Circuits* (9th Edition). Prentice Hall, 2010.
[25] C.J.M. Verhoeven, A. van Staveren, G.L.E. Monna, M.H.L. Kouwenhoven and E. Yildiz, *Structured Electronic Design: Negative Feedback Amplifiers*. Kluwer Academic, 2003.

Behzad Kazemtabrizi was born in Tehran, Iran. He received his BSc In Electrical Power Engineering from Azad University, Tehran Iran in 2006. He subsequently received his MSc and PhD degrees in Electronic and Electrical Engineering from the University of Glasgow, Scotland, UK in 2007 and 2011, respectively. He will be joining the School of Engineering and Computer Science in Durham University as a Research Associate in January 2012. He has been a graduate student member of IEEE since 2007.

Enrique Acha (SM'02) was born in Mexico. He graduated from the Universidad Michoacana de San Nicolas de Hidalgo in 1979 and obtained his PhD degree from the University of Canterbury, Christchurch, New Zealand, in 1988. He was the Professor of Electrical Power Systems at the University of Glasgow, UK in the period 2001-2011 and he is now the Professor of Electrical Power Systems at Tampere University of Technology (TUT), Finland. He is an IEEE PES distinguished lecturer.